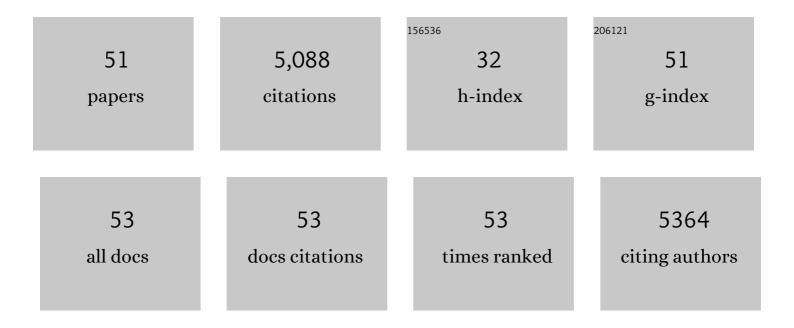
## Raphaële Clément

List of Publications by Year in descending order

Source: https://exaly.com/author-pdf/4124747/publications.pdf Version: 2024-02-01



#	Article	IF	CITATIONS
1	Role of Electron-Deficient Imidazoles in Ion Transport and Conductivity in Solid-State Polymer Electrolytes. Macromolecules, 2022, 55, 971-977.	2.2	5
2	Design of Polymeric Zwitterionic Solid Electrolytes with Superionic Lithium Transport. ACS Central Science, 2022, 8, 169-175.	5.3	54
3	Solid Electrolytes in the Spotlight. Chemistry of Materials, 2022, 34, 463-467.	3.2	4
4	High-Voltage Reactivity and Long-Term Stability of Cation-Disordered Rocksalt Cathodes. Chemistry of Materials, 2022, 34, 1524-1532.	3.2	5
5	Stacking Faults Assist Lithium-Ion Conduction in a Halide-Based Superionic Conductor. Journal of the American Chemical Society, 2022, 144, 5795-5811.	6.6	50
6	Importance of Superstructure in Stabilizing Oxygen Redox in P3â€Na <sub>0.67</sub> Li <sub>0.2</sub> Mn <sub>0.8</sub> O <sub>2</sub> . Advanced Energy Materials, 2022, 12, .	10.2	25
7	Lattice Dynamics in the NASICON NaZr <sub>2</sub> (PO <sub>4</sub> ) <sub>3</sub> Solid Electrolyte from Temperature-Dependent Neutron Diffraction, NMR, and Ab Initio Computational Studies. Chemistry of Materials, 2022, 34, 4029-4038.	3.2	6
8	Unlocking New Redox Activity in Alluaudite Cathodes through Compositional Design. Chemistry of Materials, 2022, 34, 4088-4103.	3.2	5
9	Impact of Side Chain Chemistry on Lithium Transport in Mixed Ion–Electron-Conducting Polymers. Chemistry of Materials, 2022, 34, 4672-4681.	3.2	9
10	Exceptional Cycling Performance Enabled by Local Structural Rearrangements in Disordered Rocksalt Cathodes. Advanced Energy Materials, 2022, 12, .	10.2	15
11	Polymer Electrolyte Based on Cyano-Functionalized Polysiloxane with Enhanced Salt Dissolution and High Ionic Conductivity. Macromolecules, 2022, 55, 5723-5732.	2.2	5
12	Cation-disordered rocksalt-type high-entropy cathodes for Li-ion batteries. Nature Materials, 2021, 20, 214-221.	13.3	290
13	Glass Transition Temperature and Ion Binding Determine Conductivity and Lithium–Ion Transport in Polymer Electrolytes. ACS Macro Letters, 2021, 10, 104-109.	2.3	38
14	Optimum in ligand density for conductivity in polymer electrolytes. Molecular Systems Design and Engineering, 2021, 6, 1025-1038.	1.7	0
15	A stable cathode-solid electrolyte composite for high-voltage, long-cycle-life solid-state sodium-ion batteries. Nature Communications, 2021, 12, 1256.	5.8	110
16	Formation of LiF Surface Layer During Direct Fluorination of High-Capacity Co-Free Disordered Rocksalt Cathodes. ACS Applied Materials & Interfaces, 2021, 13, 38221-38228.	4.0	13
17	Exposure History and its Effect Towards Stabilizing Li Exchange Across Disordered Rock Salt Interfaces. ChemElectroChem, 2021, 8, 3982-3991.	1.7	4
18	Probing reaction processes and reversibility in Earth-abundant Na <sub>3</sub> FeF <sub>6</sub> for Na-ion batteries. Physical Chemistry Chemical Physics, 2021, 23, 20052-20064.	1.3	5

Raphaële Clément

#	Article	IF	CITATIONS
19	Realizing continuous cation order-to-disorder tuning in a class of high-energy spinel-type Li-ion cathodes. Matter, 2021, 4, 3897-3916.	5.0	32
20	Design Principles for High-Capacity Mn-Based Cation-Disordered Rocksalt Cathodes. CheM, 2020, 6, 153-168.	5.8	103
21	Increasing Capacity in Disordered Rocksalt Cathodes by Mg Doping. Chemistry of Materials, 2020, 32, 10728-10736.	3.2	21
22	Rechargeable Batteries from the Perspective of the Electron Spin. ACS Energy Letters, 2020, 5, 3848-3859.	8.8	41
23	Redox Behaviors in a Li-Excess Cation-Disordered Mn–Nb–O–F Rocksalt Cathode. Chemistry of Materials, 2020, 32, 4490-4498.	3.2	37
24	The interplay between thermodynamics and kinetics in the solid-state synthesis of layered oxides. Nature Materials, 2020, 19, 1088-1095.	13.3	129
25	Ultrahigh power and energy density in partially ordered lithium-ion cathode materials. Nature Energy, 2020, 5, 213-221.	19.8	158
26	Cation-disordered rocksalt transition metal oxides and oxyfluorides for high energy lithium-ion cathodes. Energy and Environmental Science, 2020, 13, 345-373.	15.6	301
27	<i>Ab initio</i> computation for solid-state <sup>31</sup> P NMR of inorganic phosphates: revisiting X-ray structures. Physical Chemistry Chemical Physics, 2019, 21, 10070-10074.	1.3	10
28	Computational Investigation and Experimental Realization of Disordered High-Capacity Li-Ion Cathodes Based on Ni Redox. Chemistry of Materials, 2019, 31, 2431-2442.	3.2	50
29	Improved Cycling Performance of Liâ€Excess Cationâ€Disordered Cathode Materials upon Fluorine Substitution. Advanced Energy Materials, 2019, 9, 1802959.	10.2	127
30	Reversible Mn2+/Mn4+ double redox in lithium-excess cathode materials. Nature, 2018, 556, 185-190.	13.7	525
31	Sr3Ir2O7F2 : Topochemical conversion of a relativistic Mott state into a spin-orbit driven band insulator. Physical Review B, 2018, 98, .	1.1	3
32	Short-Range Order and Unusual Modes of Nickel Redox in a Fluorine-Substituted Disordered Rocksalt Oxide Lithium-Ion Cathode. Chemistry of Materials, 2018, 30, 6945-6956.	3.2	72
33	Design principles for high transition metal capacity in disordered rocksalt Li-ion cathodes. Energy and Environmental Science, 2018, 11, 2159-2171.	15.6	123
34	A Firstâ€Principles and Experimental Investigation of Nickel Solubility into the P2 Na <i><sub>x</sub></i> CoO <sub>2</sub> Sodiumâ€lon Cathode. Advanced Energy Materials, 2018, 8, 1801446.	10.2	34
35	A New Strategy for Highâ€Voltage Cathodes for Kâ€lon Batteries: Stoichiometric KVPO <sub>4</sub> F. Advanced Energy Materials, 2018, 8, 1801591.	10.2	130
36	Direct evidence for high Na <sup>+</sup> mobility and high voltage structural processes in P2-Na <sub>x</sub> [Li <sub>y</sub> Ni <sub>z</sub> Mn <sub>1â^'yâ^'z</sub> ]O <sub>2</sub> (x, y, z ≤) cathodes from solid-state NMR and DFT calculations. Journal of Materials Chemistry A, 2017, 5, 4129-4143.	5.2	105

Raphaële Clément

#	Article	IF	CITATIONS
37	Exploring Oxygen Activity in the High Energy P2-Type Na <sub>0.78</sub> Ni <sub>0.23</sub> Mn <sub>0.69</sub> O <sub>2</sub> Cathode Material for Na-Ion Batteries. Journal of the American Chemical Society, 2017, 139, 4835-4845.	6.6	363
38	Floating zone growth of α-Na0.90MnO2 single crystals. Journal of Crystal Growth, 2017, 459, 203-208.	0.7	6
39	Mitigating oxygen loss to improve the cycling performance of high capacity cation-disordered cathode materials. Nature Communications, 2017, 8, 981.	5.8	197
40	Insights into the Nature and Evolution upon Electrochemical Cycling of Planar Defects in the β-NaMnO <sub>2</sub> Na-Ion Battery Cathode: An NMR and First-Principles Density Functional Theory Approach. Chemistry of Materials, 2016, 28, 8228-8239.	3.2	58
41	Structurally stable Mg-doped P2-Na <sub>2/3</sub> Mn <sub>1â<sup>~</sup>y</sub> Mg <sub>y</sub> O <sub>2</sub> sodium-ion battery cathodes with high rate performance: insights from electrochemical, NMR and diffraction studies. Energy and Environmental Science, 2016, 9, 3240-3251.	15.6	264
42	The 2015 F. M. Becket Summer Research Fellowship Summary Report: In Situ NMR Study of Paramagnetic Na-Ion Battery Cathode Materials: A Challenging Experiment. Electrochemical Society Interface, 2015, 24, 74-75.	0.3	1
43	Review—Manganese-Based P2-Type Transition Metal Oxides as Sodium-Ion Battery Cathode Materials. Journal of the Electrochemical Society, 2015, 162, A2589-A2604.	1.3	386
44	Identifying the Structure of the Intermediate, Li <sub>2/3</sub> CoPO <sub>4</sub> , Formed during Electrochemical Cycling of LiCoPO <sub>4</sub> . Chemistry of Materials, 2014, 26, 6193-6205.	3.2	54
45	β-NaMnO <sub>2</sub> : A High-Performance Cathode for Sodium-Ion Batteries. Journal of the American Chemical Society, 2014, 136, 17243-17248.	6.6	333
46	Characterising local environments in high energy density Li-ion battery cathodes: a combined NMR and first principles study of LiFe <sub>x</sub> Co <sub>1â^'x</sub> PO <sub>4</sub> . Journal of Materials Chemistry A, 2014, 2, 11948-11957.	5.2	50
47	Identifying the Critical Role of Li Substitution in P2–Na <sub><i>x</i></sub> [Li <sub><i>y</i></sub> Ni <sub><i>z</i></sub> Mn <sub>1–<i>y</i>–<i>z</i>&lt; (0 &lt; <i>x</i>, <i>y</i>, <i>z</i> &lt; 1) Intercalation Cathode Materials for High-Energy Na-Ion Batteries. Chemistry of Materials, 2014, 26, 1260-1269.</sub>	/syb>]0<:	sub}2
48	Frequency-stepped acquisition in nuclear magnetic resonance spectroscopy under magic angle spinning. Journal of Chemical Physics, 2013, 138, 114201.	1.2	40
49	Density Functional Theory-Based Bond Pathway Decompositions of Hyperfine Shifts: Equipping Solid-State NMR to Characterize Atomic Environments in Paramagnetic Materials. Chemistry of Materials, 2013, 25, 1723-1734.	3.2	113
50	Hybrid Polyoxovanadates: Anion-Influenced Formation of Nanoscopic Cages and Supramolecular Assemblies of Asymmetric Clusters. Inorganic Chemistry, 2012, 51, 19-21.	1.9	37
51	Spin-Transfer Pathways in Paramagnetic Lithium Transition-Metal Phosphates from Combined Broadband Isotropic Solid-State MAS NMR Spectroscopy and DFT Calculations. Journal of the American Chemical Society, 2012, 134, 17178-17185.	6.6	122